

Numerical Investigations of MWCNT Nanofluid Cooling in Pinfin Enabled Microchannel Heat Sinks

Sorna Latha¹, Ankush D Tharkar², and Divya Haridas^{1*}

¹Department of Condensed Matter Physics, Saveetha School of Engineering, Chennai, India

²School of Mechanical Engineering, VIT Bhopal University, Bhopal India

Abstract. A numerical investigation was carried out to analyze the thermal and hydraulic performance of microchannel heat sinks (MCHSs) with varying pin heights (6.2 μm , 18.6 μm , 31 μm , and 43.4 μm) using MWCNT/water nanofluids for different volume concentrations. Simulations were performed under steady laminar flow conditions to evaluate temperature distribution, Nusselt number (Nu), friction factor (f), and thermal performance factor (TPF). Results revealed that both increasing pin height and nanofluid concentration enhanced heat transfer due to improved mixing and higher thermal conductivity. However, taller pin fins caused higher pressure drops, reducing overall hydraulic efficiency. Among all configurations, the 6.2 μm pin height with 2.5% MWCNT nanofluid pulled off the best balance between heat transfer and flow resistance, exhibiting the highest TPF across all velocities. This indicates that moderate fin height and optimal nano-particle concentration significantly improve thermal performance without excessive pumping penalties. The optimized configuration is highly compatible for compact electronic cooling and microscale thermal management systems, where efficient heat removal and minimal energy loss are indispensable.

1. Introduction

Coupled with the increasing power density of microprocessors and compact power electronics, continuous miniaturization has led to an increase in the heat generated per unit area. Efficient thermal management is thus necessary for ensuring device reliability and preventing thermal failure, as well as maintaining stable operations of the devices. Conventional cooling methods are usually not suitable for the microsystems of today because of their restricted heat dissipation capability and larger form factors. Therefore, there is a great demand for high performance and efficient cooling systems in very compact configurations that can manage high heat flux within limited spaces.

Within the last two decades, microchannel heat sinks have emerged as one of the most promising cooling solutions for high performance electronics. Their compact design, large surface area to volume ratio, and excellent convective heat transfer capability drive them to be ideal candidates for advanced thermal management applications. Tuckerman and Pease (1981) [1] pioneered microchannel based cooling by developing the first water-cooled microchannel heat sink for VLSI circuits, demonstrating that enhanced convective heat transfer in laminar flow can significantly reduce thermal resistance, achieving 790 W/cm² heat flux with a 71 °C substrate temperature rise. Compact microchannel analytical models and some optimisation algorithms were further developed by Weisberg et al. (1992) [2], who balanced the high surface area with fluid friction losses. By altering the geometry into wavy, helical, and fractal configurations that produce secondary flow and enhance fluid mixing, additional changes have been made to improve the performance of the microchannel. According to Hussein (2024) [3] numerical analysis of a mini-channel heat sink with L-shaped passages the JMMLCCHS configuration outperformed traditional rectangular ones in terms of thermal performance and resistance. Similar to this, Zhu (2024) [4] suggested

* Corresponding author: divyaharidas.sse@saveetha.com

symmetric wavy microchannels with slanted secondary channels (SW-TC), which enhanced thermal performance and flow uniformity by reducing boundary layer growth and entropy generation.

Micro-pin fins and surface-enhanced structures have been added to MCHSs to increase surface area and encourage flow mixing in order to further improve heat transfer without using excessive pumping power. Despite increased friction, Xie et al. (2021) [5] discovered that a 30° in-line pin-fin configuration generated stronger secondary flow, improving heat transfer. Similar to this, Ali et al. (2024) [6] analysed semi-elliptical pin fins ($\Psi = 0.36\text{--}1.0$) at Reynolds numbers ranging from 100 to 900 and found that the increased localised turbulence and extended surface area in an alternative arrangement significantly improved thermal performance. At $\Psi = 1.0$ and $Re = 300$, the highest overall performance (THPP = 1.41) was attained. In their comparison of various pin-fin geometries, Singh et al. (2025) [7] discovered that the circular fin provides the greatest thermal enhancement, while the triangular and square fins produce moderate enhancements. Pin-fin shape and arrangement have a significant impact on Nusselt number and pressure drop, as confirmed by Polat et al. (2022) [8]. This emphasises the need for optimised fin geometry to balance heat transfer and flow resistance. Concurrently, suspensions of nanoparticles in base fluids, or nanofluids, have drawn interest for improving the heat transfer and thermal conductivity of traditional coolants. Although higher concentrations increase viscosity and pumping power, Maheshwary et al. (2017) [9] discovered that TiO₂-water nanofluids exhibit higher thermal conductivity with increasing concentration, smaller particle size, and cubic shape. Using Al₂O₃- and diamond-water nanofluids, Hung et al. (2012) [10] reported a 20% increase in heat transfer. Murali Krishna et al. (2020) [11] demonstrated that Hybrid MWCNT-CuO/water nanofluids perform better than mono nanofluids with better heat transfer and reduced thermal resistance.

In an attempt to achieve the best MCHS performance, additional recent attempts have also been made to combine artificial intelligence methods with numerical simulation. After reviewing numerical techniques for microscale heat transfer analysis, including CFD, Lattice Boltzmann Method, and Molecular Dynamics, Gao et al. (2022) [12] came to the conclusion that CFD is still the most adaptable when working with laminar flow systems. According to Said et al. (2022) [13] MWCNT/water nanofluid enhanced shell-and-tube heat exchanger performance, increasing thermal conductivity by 3.23% and heat transfer coefficient by 31.08% at 0.3% volume fraction and the Semicircular baffles further increased efficiency by 15.4%.

In hybrid systems like PVT modules, different nanofluid-based MCHS technologies have been implemented in addition to conventional electronics cooling. According to Rajamony et al. (2024) [14], the PVT system's thermal and electrical efficiencies are increased when MWCNT-based phase change materials are incorporated. Even with these important advancements, there are still a lot of important research gaps. The improvement in heat transfer and the corresponding increase in pumping power and pressure drop have not yet been properly balanced. It is also crucial to conduct more research on the synergy of hybrid nanofluids at various concentrations with fin geometry for a variety of flow regimes. The potential for real-time design improvement and performance prediction under a variety of operating conditions is enormous when using machine learning and predictive optimisation tools. By using a numerical approach for the thermo-hydraulic performances of MCHSs with MWCNT-based nanofluids in different pin-fin geometries and configurations, the current study aims to address these issues. In order to maximise geometric and fluid parameters and improve cooling efficiency at the lowest possible energy consumption, the work methodically investigates flow and heat transfer characteristics. Thus, it is anticipated that this research will aid in the creation of next-generation micro-channel heat sinks for thermal management and high-power-density electronics.

2. Methodology

2.1 Computational Domain and Setup

ANSYS Workbench (Design Modeler) was used to simulate an MCHS for studying the laminar fluid flow and heat transfer phenomena for a number of different pin-fin geometries using various MWCNT-water nanofluid concentrations. Silicon was used as the Channel material, owing to its extremely high thermal conductivity value and structural stability. The microchannel dimensions are very small in such a way it owes to less computational cost while preserving flow and thermal accuracy. The channel with length 600 μm , width 265 μm , and height 62 μm (Table 1) and 55 cylindrical pin fins 15 μm in diameter and pitched 50 μm apart of varying height - 6.2, 18.6, 31, and 43.4 μm for studying aspect ratio effects.

The working fluids were water and MWCNT-water nanofluids at volume concentrations of 1.5% and 2.5%. Steady-state laminar conditions were used to simulate various inlet velocities between 0.5 and

2.0 m/s. At the inlet, the velocity was constant, and at the outlet, zero-gauge pressure was applied. All other walls were adiabatic, but the channel base had a constant wall heat flux. Grid independence was verified and boundary layers and fin regions were resolved using a reasonably structured mesh. ANSYS Fluent has been used to solve the governing equations of mass, momentum, and energy equations using the finite volume method. Additionally, it provides a solid foundation for optimising MCHS thermal performances with MWCNT nanofluids by shedding light on the intricate microscale flow behaviour, temperature distribution, and fluid-solid interactions.

Table 1: Channel Descriptions

Parameter	Values
Channel Length	600 μm
Channel Width	265 μm
Channel Height	62 μm
Hydraulic Diameter	100.5 μm
Pin Diameter	15 μm
Pin Spacing	50 μm
Number of Pins	55
Pin fin Height	6.2, 18.6, 31.0, 43.4 μm
Nanofluid	MWCNT
Nanofluid Concentration	1.5% and 2.5%

2.2 Material and Fluid Characteristics:

The thermal performance of the MCHS strongly depend on the thermophysical properties of both the working fluid and the substrate material. In this study, deionized water and MWCNT–water nanofluids with 1.5% and 2.5% volume concentrations were used as coolants, while aluminium served as the channel substrate.

Water was selected as the base fluid since it has high specific heat, moderate thermal conductivity, and low viscosity, all of which promote effective convective cooling. By using Brownian motion and micro-convection effects, the addition of MWCNT nanoparticles improves the fluid's effective thermal conductivity and temperature uniformity. Table 2 summarises each working fluid's thermophysical characteristics. Because of its high thermal conductivity (386 W/m·K), low density, and good mechanical stability, aluminium was chosen for its ability to spread heat quickly and withstand repeated thermal cycling. By reducing thermal resistance and improving the overall cooling efficiency of the MCHS, the combination of MWCNT-water nanofluids and an aluminium substrate offers superior heat removal and uniform temperature distribution.

Table 2: Properties of the Materials

<i>Thermo-Physical Properties</i>	<i>Water</i>	<i>MWCNT</i>	<i>Aluminium</i>
Density (kg/m ³)	997	1600	2700
Dynamic Viscosity (kg/m·s)	0.000891	-	-
Thermal Conductivity (W/m·K)	0.6	3000	386
Specific Capacitance (J/kg·K)	4182	796	903

2.3 Computational Setup and Boundary Conditions:

The thermal and flow behavior of the MCHS is analyzed numerically using a well-structured simulation setup and clearly specified boundary conditions. As can be seen from Table 3, at the channel entrance, a uniform inlet velocity is imposed for four flow rates: 0.5, 1.0, 1.5, and 2.0 m/s corresponding to Reynolds numbers within the range of 56 to 225, representing laminar flow in microchannels. The temperature of water and MWCNT/water nanofluids with 1.5% and 2.5% concentrations is kept the same by maintaining a fixed value of inlet temperature at 300 K to ensure uniformity of the initial conditions. A zero-gauge pressure at the outlet is taken into consideration in order to simulate the case of atmospheric discharge realistically while ensuring proper pressure drop in the flow direction.

A constant heat flux of 10 kW/m² is applied to the bottom wall of the channel, to represent the heat generated from electronic components, while the other three walls are treated as adiabatic to prevent heat loss. All solid–fluid interfaces are modeled with no-slip boundary conditions to capture the viscous effects properly.

These simulations are performed using ANSYS Fluent software by applying the Finite Volume Method. The SIMPLE algorithm is adopted to couple pressure and velocity, while a second-order upwind scheme is adopted for the convective terms to enhance the numerical resolution. In solving these problems, the convergence criteria are set, with residuals less than 10⁻⁶ for continuity and momentum equations, while the energy equations are less than 10⁻⁹. These configurations guarantee dependable and stable computation.

Table 3: Boundary conditions

Boundary Conditions	Values
Inlet Velocity	0.5 - 2 m/s
Inlet Temperature	300 K
Outlet Pressure	0 Pas
Heat Flux	10 kW/m ²
Reynolds Numbers	56.23, 112.5, 168.7, 225
Flow Type	Laminar

2.4. Mathematical model:

Steady-state laminar flow and conjugate heat transfer in the microchannel are modeled using 3D continuity, momentum, and energy equations applied to both fluid and solid domains.

Continuity

$$\nabla \cdot \vec{u} = 0 \tag{1}$$

Momentum

$$\rho_l (\vec{u} \cdot \nabla \vec{u}) = -\nabla p + \mu_l \nabla^2 \vec{u} \tag{2}$$

Energy

$$\rho_l C_{pl} (\vec{u} \cdot \nabla T_l) = k_l \nabla^2 T \tag{3}$$

Energy (solid)

$$\nabla (k_s \cdot \nabla T_s) = 0 \tag{4}$$

Numerical Calculations:

Hydraulic Diameter (D_h):

$$D_h = \frac{4(W_{ch} \times H_{ch})}{2(W_{ch} + H_{ch})} \tag{5}$$

Where H_{ch} - Height and W_{ch} - width

Reynolds number (Re):

$$Re = \frac{\rho u D_h}{\mu_l} \tag{6}$$

Heat transfer coefficient (h):

$$h = \frac{q}{T_w - T_f} \tag{7}$$

Nusselt number (Nu):

$$Nu = \frac{hD_h}{k} \quad (8)$$

Friction factor (f):

$$f = \frac{2D_h \Delta p}{L \rho u_{in}^2} \quad (9)$$

Thermal Performance Factor (TPF):

$$TPF = \frac{Nu/Nu_0}{(f/f_0)^{1/3}} \quad (10)$$

Nanofluid Properties:

Density:[15]

$$\rho_{nf} = (1 - \phi) \rho_{bf} + \phi \cdot \rho_p$$

Viscosity: (Brinkman - model)

$$\mu = \frac{\mu_{bf}}{(1 - \phi)^{2.5}}$$

Thermal Conductivity: (Hamilton - Crosser)

$$k_{nf} = k_{bf} \frac{k_s + (n-1) k_{bf} - (n-1) \phi (k_s - k_{bf})}{k_s + (n-1) k_{bf} + \phi (k_s - k_{bf})}$$

Specific Heat Capacity:

$$C_{pnf} = \frac{(1 - \phi) \rho_{bf} C_{bf} + \phi \rho_p C_p}{\rho_{nf}}$$

3. Result and Discussion:

3.1. Flow Field Analysis: Velocity Streamlines and Vectors

The flow characteristics for a pin fin height of 6.2 μm at an inlet velocity of 2 m/s were analyzed through the velocity streamline and vector plots taken at a plane close to the pin height to visualize the interruption caused by the fins

(a) Velocity Streamlines

The velocity streamline distribution for a pin fin height of 6.2 μm at an inlet velocity of 2 m/s is shown in Figure 1(a). Because of flow obstruction and separation, there is noticeable streamline distortion around the pin surfaces, but the flow is still fairly uniform in the inter-fin regions. The pin fins act as micro-scale vortex generators, which enhance the mixing between the fluid layers adjacent to the heated walls and the bulk flow.

The color contour indicates velocity magnitudes with elevated values observed in the narrow gaps between adjacent pins. This local acceleration increases the velocity gradient near the wall, which is beneficial for convective heat transfer. However, the formation of low velocity wake zones behind each pin fin suggests the onset of re-circulation regions. These wakes reduce momentary local heat transfer coefficients, but the repeated interruption of boundary layers across successive rows enhances overall heat transfer performance.

A balanced trade-off between fluid disturbance and pressure loss is shown by the streamline pattern for the 6.2 μm fin height. The shorter fin height results in milder flow deflection than taller pin fins (e.g., 18.6 μm or 31 μm), which reduces frictional losses while maintaining enough turbulence intensity to enhance heat transfer. This finding is consistent with the Thermal Performance Factor (TPF) results, which showed that the 6.2 μm configuration performed best at moderate Reynolds numbers ($Re \approx 112-168$).

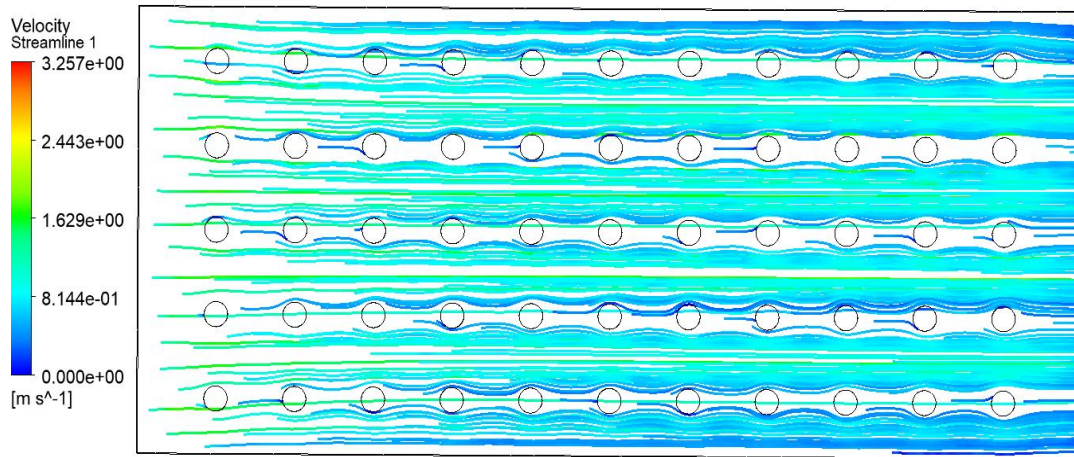


Fig 1 (a). Velocity Streamlines of pin height $6.2 \mu\text{m}$ at a velocity of 2 m/s

(b) Velocity Vectors

The velocity vector plot for the same configuration is shown in Figure 1(b). Wake zones, where velocity vectors reverse direction and create tiny re-circulation bubbles, are clearly visible downstream of each pin fin in the vector field. These tiny vortices periodically shed, which increases the effective thermal boundary layer disruption and causes unsteady mixing.

The vectors demonstrate a considerable fluid acceleration around the pin sides, especially in the vicinity of the top rows, which causes a localised increase in shear rate. Elevated convective heat transfer coefficients are correlated with this increased shear. The low-velocity zones behind the pins, on the other hand, represent stagnation and flow separation points, which are required to sustain efficient turbulence-driven heat transfer enhancement but are linked to somewhat higher pressure drops. According to the flow structure, the microchannel functions in a laminar-to-transitional regime at 2 m/s , where vortex formation and reattachment control the flow behaviour. The pin array functions as a flow interrupter, continuously renewing the boundary layer, as confirmed by the periodic nature of the velocity vectors. This behavior supports numerical findings that the inclusion of pin fins at moderate heights and flow velocities enhances both the Nusselt number and the overall TPF, without imposing excessive frictional penalties.

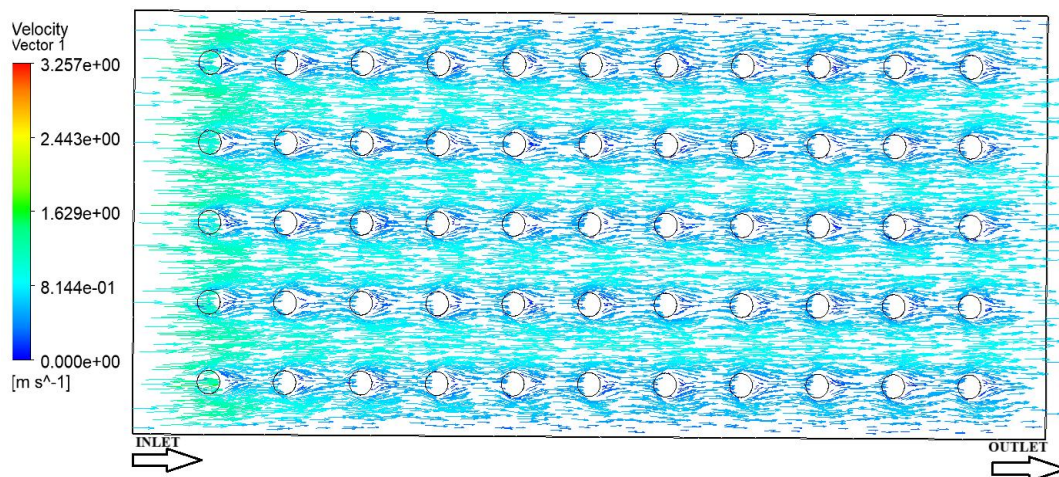


Fig 1 (b). Velocity Vector of the pin height $6.2 \mu\text{m}$ at a velocity of 2 m/s

3.2. Temperature Contour:

The temperature contour shown corresponds to the $6.2 \mu\text{m}$ pin height at a velocity of 2 m/s is shown in Fig 2. To accurately depict the impact of the fins on the local thermal field, the contour is taken at a plane near the pin height. The temperature distribution shows uniform spreading throughout the flow path and a

smooth gradient from the inlet to the outlet. By upsetting the thermal boundary layer, the pins facilitate improved mixing and heat transfer between the heated surface and the fluid. The comparatively short pin height in this arrangement minimizes excessive pressure loss while enabling sufficient fluid circulation around the fins. In line with the higher Thermal Performance Factor (TPF) noted for the 6.2 μm case, this balance produces a uniform temperature field and effective convective heat transfer. In contrast, simulation data show higher local temperature gradients for higher pin heights (18.6 μm , 31 μm , and 43.4 μm) because of stronger wake formation and re-circulation zones behind the pins. The stronger flow obstruction causes higher pressure drops and a corresponding decrease in overall efficiency, even though these configurations show higher Nusselt numbers.

As a result, the pin height of 6.2 μm exhibits the best thermal performance, combining efficient heat removal with steady flow behaviour that is consistent with the velocity field and TPF trends.

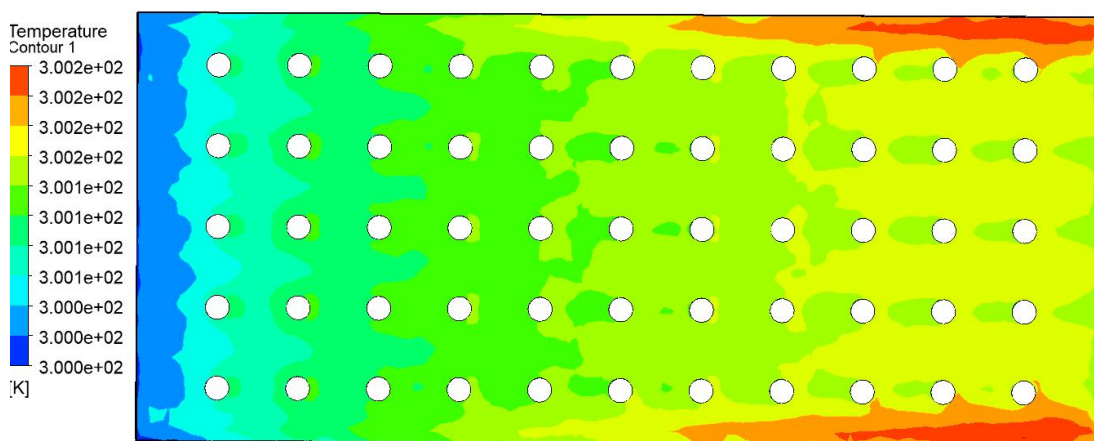


Fig 2. Temperature contour of the pin 6.2 μm with 2 m/s velocity

3.3. Friction Factor Analysis:

Figure 3 shows how the friction factor (f) varies with Reynolds number (Re) for various pin heights and nanofluid concentrations. The laminar flow behaviour characteristic of microchannel configurations is confirmed by the results, which unequivocally show that the friction factor consistently decreases with increasing Reynolds number in all the cases. Higher friction losses result from the flow being more affected by surface interactions and viscous effects at lower Re values. The viscous boundary layer thins and the relative impact of wall shear decreases as Re rises, which lowers f .

The water-cooled microchannel has the highest friction factor at $Re = 56.23$, which ranges from 0.83 for the plain channel to 2.50 for the 43.4 μm pin height. It then gradually drops to 0.25–0.70 at $Re = 225$. This pattern demonstrates that the addition of pin fins increases pressure loss and flow disturbance because of the increased surface area and form drag. The plain channel has the least amount of frictional resistance, while the 43.4 μm fins have the biggest pressure drop and the highest f values among all pin-fin heights. A small increase in f is seen when using MWCNT–water nanofluids as opposed to pure water under comparable circumstances, which is explained by the increase in effective viscosity brought on by the suspension of nanoparticles.

This increase is still modest, though, suggesting that the nanofluid improves heat transfer without causing appreciable hydraulic penalties. The friction factor for the 1.5% MWCNT concentration ranges from 0.78 to 2.35 at low Re and decreases to 0.21 to 0.67 at higher Re . The viscosity enhancement brought on by the higher particle volume fraction is consistent with the 2.5% MWCNT nanofluid's similar trend, albeit with slightly higher values at lower Reynolds numbers.

When comparing pin heights, f rises with fin height because of increased flow path obstruction, which increases form drag and flow recirculation around the pin bases. While 6.2 μm fins offer a balanced performance between pressure drop and flow mixing, 43.4 μm fins consistently exhibit the highest friction factors. The friction factor for 43.4 μm fins with 2.5% MWCNT is 0.678 at $Re = 225$, which is almost three times greater than the plain channel value (0.21) under the same circumstances.

Overall, the trends in the friction factor confirm that, although hydraulic resistance is slightly increased by increasing pin-fin height and nanofluid concentration, this increase is within acceptable

bounds for microscale cooling systems. According to the results, MWCNT–water nanofluids with optimised pin-fin geometries are an effective solution for microchannel heat sink applications because the thermal performance gains obtained through surface enhancement and nanofluid usage outweigh the slight increase in flow resistance.

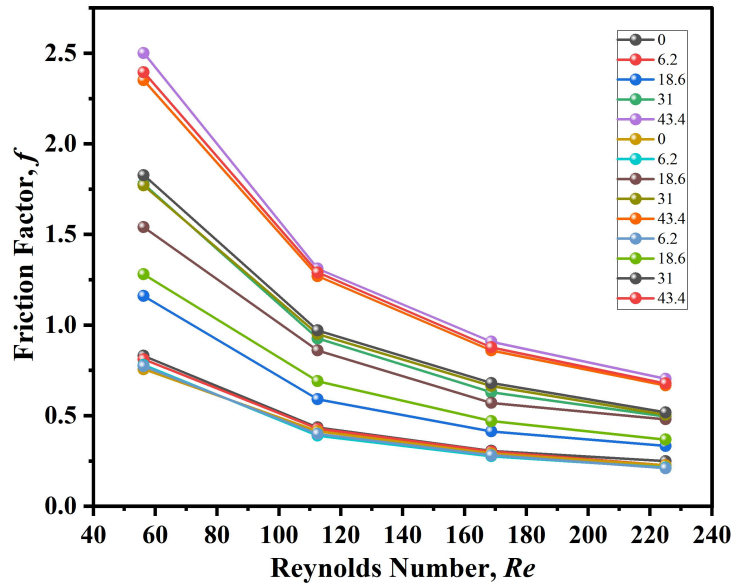


Fig 3: Friction Factor vs Reynolds Number

3.4. Nusselt Number:

The Nusselt number trends (Fig. 4) show a consistent improvement in convective heat transfer with increasing Reynolds number. Nu increases for the plain channel from ≈ 4.3 at $Re = 56$ to ≈ 6.9 at $Re = 225$, which is consistent with classical laminar scaling, in which higher bulk velocity increases convective transport and thins the thermal boundary layer. For the same Reynolds numbers, adding pin fins greatly increases Nu; for instance, 43.4 μm fins yield the biggest improvement, with Nu values higher than the plain channel by about 10–30% depending on Re and concentration. Increased wetted surface area, flow separation and reattachment, and stronger secondary flows surrounding the pins, which continuously replenish the near-wall fluid and lower thermal resistance are responsible for this improvement.

Nu is also positively impacted by nanofluid concentration. At the same Re and geometry, the Nusselt numbers of 1.5% and 2.5% MWCNT suspensions are higher than those of pure water. For the largest pin heights, the 2.5% cases show the highest Nu (up to $\approx 8-9$ at $Re \approx 225$), which is consistent with improved micro-scale energy transport by nanoparticles (Brownian motion and micro-convection) and enhanced effective thermal conductivity. Pin geometry and nanofluid loading work together to produce the strongest Nu increases for tall-pin + 2.5% MWCNT cases. Taller pins increase mixing and surface area, while higher particle loading enhances heat-carrying capacity.

Nu increases are more noticeable at higher Re, suggesting that as convective transport intensifies, geometric enhancements produce a larger relative benefit. However, at the highest Re, the relative Nu gain from increasing pin height slightly decreases, indicating a limit to mixing benefits as the boundary layer gets extremely thin. Optimization must weigh increased heat transfer against pumping power because, when comparing thermal gain to hydraulic penalty, the highest Nu values correspond with the largest friction-factor increases (e.g., 43.4 μm at 2.5% MWCNT). Overall, the findings demonstrate that for microchannel heat sinks with reasonable hydraulic costs, customized pin-fin designs in conjunction with moderate MWCNT loading can produce notable convective improvement.

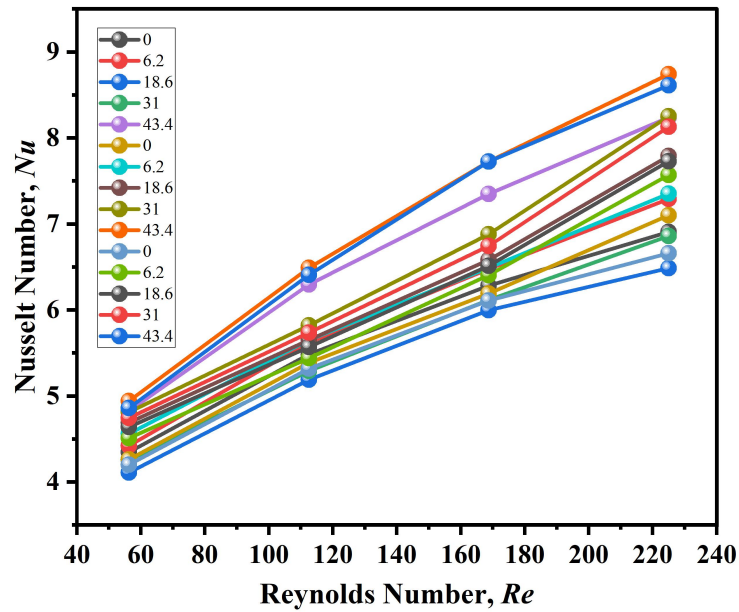


Fig 4: Nusselt number vs Reynolds number

3.5. Thermal Performance Factor:

The Thermal Performance Factor (TPF) for various working fluids varies with Reynolds number and pin-fin height. TPF is a direct measure of overall thermal-hydraulic efficiency because it combines the effects of heat transfer enhancement and the related hydraulic penalty. Physically, a TPF value larger than unity indicates that the design is energetically advantageous because the relative improvement in heat transfer exceeds the increase in pressure loss. The TPF values for all working fluids in the current study stay near or slightly above unity, indicating that the increased heat transfer made possible by pin-fin structures and nanofluid loading effectively offsets the corresponding increase in friction factor. Water and nanofluids with shorter fins (6.2 μm and 18.6 μm) have the highest TPF values ($\approx 1.03 - 1.07$) at low Reynolds numbers ($Re \approx 56$), whereas tall fins (31 – 43.4 μm) have somewhat lower values ($\sim 0.75 - 0.85$). This is due to the fact that at lower flow velocities, the convective advantage of large fins does not completely offset the increased drag, and the pressure loss contribution is dominant in channels with higher obstruction.

As the Reynolds number increases, TPF gradually improves for all fluids, indicating better heat transfer efficiency at higher flow rates. For MWCNT nanofluids, TPF values at $Re = 225$ range between 0.86 and 1.16, with the 2.5% concentration at 6.2 μm pin height showing the highest TPF (≈ 1.16) (Fig 5). This corresponds to a regime where the thermal enhancement due to improved fluid conductivity and nano particle-induced micro-convection dominates over frictional losses. The presence of nanoparticles increases the effective thermal conductivity of the fluid, enhances temperature uniformity, and promotes micro vortical motions that augment convective heat transfer, all of which contribute to elevated Nusselt numbers.

In contrast, taller fins (31 μm and 43.4 μm) have higher Nusselt numbers, but they also show larger friction factors because of increased wake formation and flow obstruction behind the pins. As a result, the corresponding TPF values ($\approx 0.79 - 0.85$) slightly decrease, highlighting the fact that when the pressure penalty outweighs the heat transfer gain, excessive pin height can result in diminishing returns. The best overall thermal performance is consistently produced by the 6.2 μm and 18.6 μm fins, which maintain an excellent balance. While preserving a comparatively smooth pressure gradient, moderate pin heights encourage enough boundary-layer disruption for efficient heat transfer. Furthermore, nanofluids containing 1.5-2.5 volume concentrations of MWCNT enhance energy transport without significantly raising viscosity, guaranteeing the flow's thermal efficiency.

In summary, the 6.2 μm pin-fin configuration with 2.5% MWCNT demonstrates the best overall thermal-hydraulic performance, achieving a favorable compromise between enhanced convective transport (high Nu) and moderate hydraulic resistance (controlled f), as reflected by the highest TPF values. This indicates that microchannel heat sinks employing moderately sized pin fins and optimized

nanofluid concentrations can achieve superior heat dissipation efficiency with acceptable pumping power requirements.

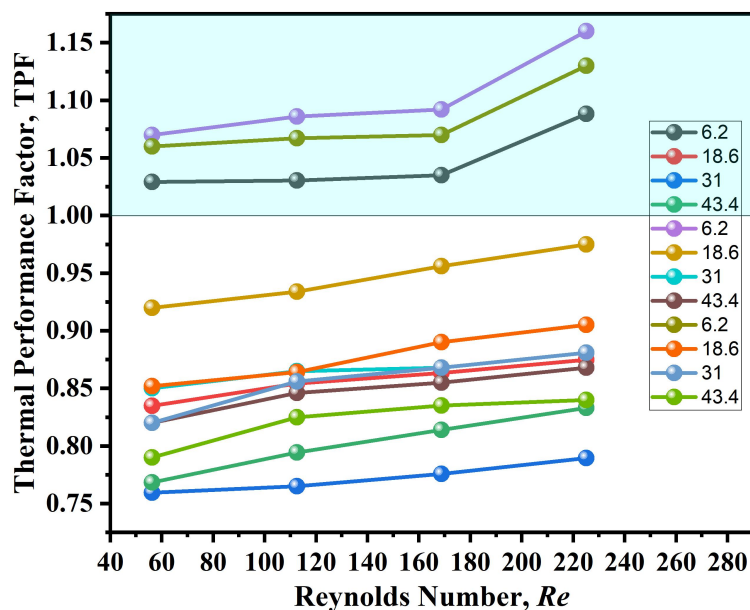


Fig 5: TPF vs Reynolds number

4. Conclusion:

The numerical investigation confirms that both pin height and MWCNT nanofluid concentration play a decisive role in determining the overall heat transfer and flow behavior within a microchannel heat sink. The increase in nanofluid concentration augments the effective thermal conductivity, which fosters stronger convection and more uniform temperature distribution across the heated surface. Similarly, higher pin heights enriches the surface area and create local flow disturbance, increasing the Nusselt number.

Nevertheless, excessive pin height also induces greater flow obstruction, resulting in higher pressure drops and friction factors, which reduce overall efficiency. From the combined analysis of Nusselt number, friction factor, and Thermal Performance Factor (TPF), it is concluded that:

- ✧ The 6.2 μm pin height yields the best thermal-hydraulic balance, producing efficient heat removal with minimal pressure penalty.
- ✧ Between the two concentrations, the 2.5% MWCNT nanofluid exhibits superior thermal performance due to enhanced thermal conductivity and particle-induced micro-convection.
- ✧ The optimum configuration is the 6.2 μm pin height with 2.5% MWCNT nanofluid, achieving high TPF values and smooth flow characteristics even at higher velocities.

This optimized microchannel design can be effectively employed in microelectronics cooling, solar thermal collectors, lab-on-chip (LOC) devices, and high-density power modules, where enhanced heat transfer and compactness are crucial for system stability and performance.

References

- [1] D.B. Tuckerman, R.F.W. Pease, High-performance heat sinking for VLSI, IEEE Electron Device Lett., **2**, 126–129 (1981).
- [2] A. Weisberg, H.H. Bau, J. Zemel, Analysis of microchannels for integrated cooling, Int. J. Heat Mass Transf., **35(10)**, 2465–2474 (1992). [https://doi.org/10.1016/0017-9310\(92\)90089-B](https://doi.org/10.1016/0017-9310(92)90089-B)

- [3] H.A. Hussein, A simulation study of thermal and hydraulic characteristics mini-channel circular heat sink: Effect of L-shaped multi-channel arrangement on flow maldistribution, *Case Stud. Therm. Eng.*, **65**, 105655 (2024). <https://doi.org/10.1016/j.csite.2024.105655>
- [4] Q. Zhu, X. Liu, J. Zeng, H. Zhao, W. He, H. Deng, G. Chen, Numerical study of heat transfer and fluid flow in a symmetric wavy microchannel heat sink reinforced by slanted secondary channels, *Case Stud. Therm. Eng.*, **65**, 105605 (2024). <https://doi.org/10.1016/j.csite.2024.105605>
- [5] G. Xie, L. Zhao, Y. Dong, Y. Li, S. Zhang, C. Yang, Hydraulic and Thermal Performance of Microchannel Heat Sink Inserted with Pin Fins, *Micromachines*, **12(3)**, 245 (2021). <https://doi.org/10.3390/mi12030245>
- [6] N. Ali, S. Srivastava, I. Haque, J. Yadav, T. Alam, T.U. Siddiqui, M.I.H. Siddiqui, E. Cuce, Heat dissipation and fluid flow in micro-channel heat sink equipped with semi-elliptical pin-fin structures: A numerical study, *Int. Commun. Heat Mass Transf.*, **155**, 107492 (2024). <https://doi.org/10.1016/j.icheatmasstransfer.2024.107492>
- [7] J. Singh, A. Garg, P. Kumar, R. Shakya, T.R. Sahu, A. Kumar, P.K. Shukla, Numerical Analysis of Laminar Flow and Heat Transfer in Micro Pin Fin Heat Sinks with Varying Fin Geometries: Effect of Fin Geometry on Micro Pin Fin Heat Sinks, *Preprints* (2025). <https://doi.org/10.20944/preprints202508.0610.v1>
- [8] M.E. Polat, F. Ulger, S. Cadirci, Multi-objective optimization and performance assessment of microchannel heat sinks with micro pin-fins, *Int. J. Therm. Sci.*, **174**, 107432 (2022). <https://doi.org/10.1016/j.ijthermalsci.2021.107432>
- [8] P. Maheshwary, C. Handa, K. Nemade, A comprehensive study of effect of concentration, particle size and particle shape on thermal conductivity of titania/water based nanofluid, *Appl. Therm. Eng.*, **119**, 79–88 (2017). <https://doi.org/10.1016/j.applthermaleng.2017.03.054>
- [9] T. Hung, W. Yan, X. Wang, C. Chang, Heat transfer enhancement in microchannel heat sinks using nanofluids, *Int. J. Heat Mass Transf.*, **55(9–10)**, 2559–2570 (2012). <https://doi.org/10.1016/j.ijheatmasstransfer.2012.01.004>
- [11] V. Murali Krishna, M. Sandeep Kumar, O. Mahesh, P. Senthil Kumar, Numerical investigation of heat transfer and pressure drop for cooling of microchannel heat sink using MWCNT-CuO-Water hybrid nanofluid with different mixture ratio, *Mater. Today Proc.*, **42**, 969–974 (2020). <https://doi.org/10.1016/j.matpr.2020.11.935>
- [12] J. Gao, Z. Hu, Q. Yang, X. Liang, H. Wu, Fluid flow and heat transfer in microchannel heat sinks: Modelling review and recent progress, *Therm. Sci. Eng. Prog.*, **29**, 101203 (2022). <https://doi.org/10.1016/j.tsep.2022.101203>
- [13] Z. Said, S. Rahman, P. Sharma, A. Amine Hachicha, S. Issa, Performance characterization of a solar-powered shell and tube heat exchanger utilizing MWCNTs/water-based nanofluids: An experimental, numerical, and artificial intelligence approach, *Appl. Therm. Eng.*, **212**, 118633 (2022). <https://doi.org/10.1016/j.applthermaleng.2022.118633>
- [14] R.K. Rajamony, J.K.S. Paw, A.K. Pandey, et al., Thermal analysis and thermal regulation of photovoltaic thermal system using serpentine tube absorber with modified multi-walled carbon nanotubes enhanced PCM, *J. Therm. Anal. Calorim.*, **149**, 14643–14662 (2024). <https://doi.org/10.1007/s10973-024-13845-7>
- [15] A. Basem, M. Abdeldayem, D.J. Jasim, H. Nabi, Exploring the efficiency of employing Fe₃O₄-MWCNT Nanofluids in a heat sink equipped with circular micro pin-fins, *Int. J. Thermofluids*, **24**, 100928 (2024). <https://doi.org/10.1016/j.ijft.2024.100928>